



## Effect of the composition of the hot product stream in the quasi-steady extinction of strained premixed flames

Bruno Coriton, Mitchell D. Smooke, Alessandro Gomez\*

Department of Mechanical Engineering, Yale Center for Combustion Studies, Yale University, New Haven, CT 06520-8286, United States

### ARTICLE INFO

#### Article history:

Received 23 February 2010

Received in revised form 16 April 2010

Accepted 1 May 2010

Available online 10 June 2010

#### Keywords:

Strained premixed flames

Extinction

Combustion products

Stratified combustion

### ABSTRACT

The extinction of premixed  $\text{CH}_4/\text{O}_2/\text{N}_2$  flames counterflowing against a jet of combustion products in chemical equilibrium was investigated numerically using detailed chemistry and transport mechanisms. Such a problem is of relevance to combustion systems with non-homogeneous air/fuel mixtures or recirculation of the burnt gases. Contrary to similar studies that were focused on heat loss/gain, depending on the degree of non-adiabaticity of the system, the emphasis here was on the yet unexplored role of the *composition* of counterflowing burnt gases in the extinction of lean-to-stoichiometric premixed flames. For a given temperature of the counterflowing products of combustion, it was found that the decrease of heat release with increase in strain rate could be either monotonic or non-monotonic, depending on the equivalence ratio  $\varphi_b$  of the flame feeding the hot combustion product stream. Two distinct extinction modes were observed: an abrupt one, when the hot counterflowing stream consists of either inert gas or equilibrium products of a stoichiometric premixed flame, and a smooth extinction, when there is an excess of oxidizing species in the combustion product stream. In the latter case four burning regimes can be distinguished as the strain rate is progressively increased while the heat release decreases smoothly: an adiabatic propagating flame regime, a non-adiabatic propagating flame regime, the so-called partially-extinguished flame regime, in which the location of the peak of heat release crosses the stagnation plane, and a frozen flow regime. The flame structure was analyzed in detail in the different burning regimes. Abrupt extinction was attributed to the quenching of the oxidation layer with the entire H–OH–O radical pool being comparably reduced. Under conditions of smooth extinction, the behavior is different and the concentration of the H radical decreases the most with increasing strain rate, whereas OH and O remain comparatively abundant in the oxidation layer. As the profile of the heat release rate thickens, the oxidation layer is quenched and the attack of the fuel relies more heavily on the OH radicals.

© 2010 The Combustion Institute. Published by Elsevier Inc. All rights reserved.

### 1. Introduction

The extinction of premixed flames is a classic combustion problem that has been tackled over the years with a variety of approaches including experimental, computational and analytical ones. For a fresh reactant/hot product counterflow system, we here take a narrow focus aimed at showing that even for such a classic problem there are still important aspects that have yet to be unveiled.

Libby and Williams [1] were the first to analyze the counterflow configuration opposing a fresh mixture to a hot stream by activation energy asymptotics with a one-step overall irreversible reaction mechanism. When the rate of heat release was plotted against the strain rate, the resulting curve exhibited either a Z-

shape or a decreasing monotonic profile that are classically referred to as the unfolded and stretched Z-curves, respectively. In regimes of unfolded Z-curves, the extinction strain rate is determined at the upper turning point between the upper and middle branches of the Z-curve, where the slope of the heat release rate with respect to the strain rate becomes vertical. The upper and lower branches of the Z-curve are stable combustion regimes whereas the middle branch corresponds to unstable burning states. At the extinction turning point, the system is expected to undergo an abrupt change of heat release with an infinitesimal increment of the strain rate. In contrast, there is no turning point of the stretched Z-curve, the heat release rate progressively decays with the strain rate and the extinction of the flame is smoothly driven by the strain rate. Those authors demonstrated that regimes of stretched Z-curve are encountered when the temperature of the counterflowing gases is near or above the adiabatic temperature of the premixed flame. As the strain increases, the flame is displaced closer to the gas stagnation plane and the flame temperature increases. The elevated temperature of the counterflowing

\* Corresponding author. Address: Department of Mechanical Engineering, Yale University, P.O. Box 208286, New Haven, CT 06520-8286, United States. Fax: +1 203 432 7654.

E-mail address: [alessandro.gomez@yale.edu](mailto:alessandro.gomez@yale.edu) (A. Gomez).

gases helps to sustain the chemical reaction rate within the flame which otherwise would not be able to maintain steady burning. They labeled such a flame as partially extinguished because of the modest heat release. Their analysis also showed that at elevated strain rates the flame crosses the stagnation plane and develops an effectively negative flame speed whereas the fuel consumption rate is still positive. Since the flame is located on the side of the stagnation plane opposite to the fresh reactant stream, the diffusive fluxes must overcome an adverse convective transport in the reaction zone. Otherwise, when the temperature  $T_b$  is below the adiabatic flame temperature, the flame loses heat as the reaction zone approaches the hot gases at the stagnation plane as a result of the increasing strain rate. Abrupt extinction is the result of too severe a heat loss of the reaction zone in the vicinity of the stagnation plane.

Darabiha et al. [2], who solved the problem numerically also using a one-step overall irreversible reaction mechanism, confirmed the existence of the partially-extinguished flame. The work of Libby and Williams [1] was also found by Darabiha et al. [3] in qualitative agreement with numerical solutions employing detailed chemical and transport mechanism for propane/air counterflow flames. In their study, the hot stream composition corresponded to the reactant mixture equilibrium composition at the temperature  $T_b$ . Rogg [4] analyzed in more detailed the effect of strain rate on the flame structure and argued that the mechanism leading to extinction was the enhanced diffusion of the H radical out of the reaction zone, toward the hot side of the flame. However, in [4], flame computations with an 18-step reaction mechanism did not illustrate the partially-extinguished regime of Libby and Williams [1]. In an added note at the end of his article, Rogg [4] mentioned that further calculations with a more detailed reaction mechanism showed a continuous decrease of the heat release with increasing rate of strain but no follow-up was ever published. The present study expands upon these findings by focusing on the role played by the composition of the counterflowing combustion products.

In the context of turbulent premixed combustion, flamelet models regard the turbulent flame front as an ensemble of stretched laminar flames [5], as depicted in Fig. 1. For the modeling of turbulent premixed flames, Libby and Williams [6] introduced the concept of adiabatic laminar counterflow premixed flamelets opposed to products of combustion. Hawkes and Chen [7] found that the reactant-to-product strained flamelet model produced results in good agreements with flame properties obtained using DNS simulations. Najm and Wyckoff [8], in a study of the interaction of toroidal vortices with premixed flames, suggested that the premixed flame is brought closer to extinction by a displacement of the reaction zone into the products of combustion. They argued that dilution of oxidizer and the reversal of the terminating reac-

tions in the chemical mechanism by the hot products of combustion leads to the extinction of the flame. Depletion of the H radical and the excess of OH radical were also pointed out near extinction. Mastorakos et al. [9] experimentally studied the blow-off of a turbulent premixed flame opposed to a jet of hot products of combustion produced by a lean methane/air flame. They reported that the premixed flame could not be extinguished by the bulk strain rate when the temperature of the hot products was greater than 1550 K.

Other studies of direct relevance are those on lean stratified premixed combustion in which burning rates of flames of different equivalence ratios can affect each other: as demonstrated by Marzouk et al. [10] and Kang and Kyritsis [11], the burning rates of the leaner flames are enhanced by back diffusion of heat from the products of combustion of flames with composition closer to stoichiometric.

In this contribution, we examined computationally how the extinction behavior of strained premixed flames is affected not only by the hot product stream temperature, which can be easily explained in terms of volumetric heat loss, but also by the hot product composition, which, in turn, is affected by the composition of the premixed flame feeding the combustion product stream (Fig. 1). We discovered this behavior serendipitously in a study of turbulent premixed flames in counterflow [12], which prompted an in-depth analysis of the laminar flame counterpart. We considered strained  $\text{CH}_4/\text{O}_2/\text{N}_2$  premixed flames counterflowing against either a combustion product stream or an inert stream and studied their extinction numerically using detailed chemistry and transport. Controlled independent variables included the fresh reactant composition, the temperature and the composition of the hot product stream. We also addressed the relevance of the present scenario to practical, and inevitably turbulent, combustion systems.

## 2. Numerical modeling and methodology

The “fresh reactants/hot products” problem was modeled as described in [13]. The elliptic form of the 2D conservation equations in cylindrical coordinates was reduced to a 1D nonlinear two-point boundary value problem by making use of a similarity transformation. The equations to be solved in 1D are given below.

$$\begin{aligned} \frac{dV}{dx} + 2\rho U &= 0, \\ \frac{d}{dx} \left( \mu \frac{dU}{dx} \right) - V \frac{dU}{dx} - \rho U^2 - J &= 0, \\ -\frac{d}{dx} (\rho Y_k V_k) - V \frac{dY_k}{dx} + \dot{\omega}_k W_k &= 0, \quad k = 1, 2, \dots, K, \\ \frac{d}{dx} \left( \lambda \frac{dT}{dx} \right) - c_p V \frac{dT}{dx} - \sum_{k=1}^K \rho Y_k V_{dk} c_{pk} \frac{dT}{dx} - \sum_{k=1}^K \dot{\omega}_k W_k h_k^0 - \nabla \cdot \vec{q}_R &= 0, \\ \frac{dj}{dx} &= 0. \end{aligned}$$

There are  $K+4$  coupled equations, where  $K$  is the number of chemical species in the mechanism. In these equations,  $x$  refers to the axial spatial coordinate;  $U$ , the radial similarity variable ( $U(x) = u(r, x)/r$ , where  $r$  and  $u$  denote the radial spatial coordinate and the radial velocity component, respectively);  $V$ , the axial mass flux;  $\rho$ , the mass density;  $\mu$ , the kinematic viscosity;  $J$ , the reduced pressure gradient;  $Y_k$ , the mass fraction of the  $k$ th species;  $\dot{\omega}_k$ , the molar rate of production per unit volume of the  $k$ th species;  $W_k$ , the molecular weight of the  $k$ th species;  $\lambda$ , the thermal conductivity of the mixture;  $T$ , the temperature;  $c_p$ , the constant-pressure heat capacity of the mixture;  $V_{dk}$ , the diffusion velocity of the  $k$ th species;  $c_{pk}$ , the constant-pressure heat capacity of the  $k$ th species;  $h_k^0$ , the enthalpy of formation of the  $k$ th species at reference tem-

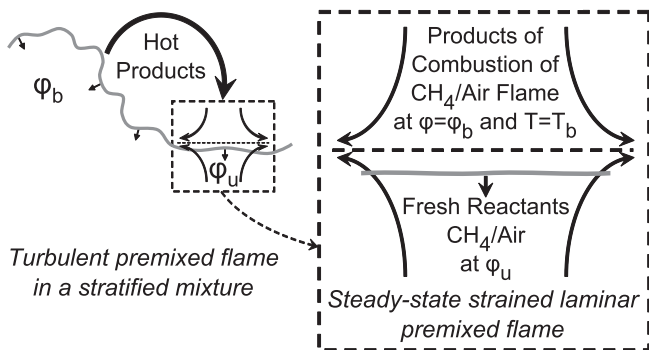


Fig. 1. Schematic of the counterflow configuration and relevance to stratified turbulent flames.

perature  $T^0$ ;  $\nabla \cdot \vec{q}_R$ , the divergence of the net radiative flux. All thermodynamic, chemical, and detailed transport properties were evaluated using optimized and highly efficient vector libraries [15]. The reduced pressure gradient  $J$ , denoted by  $J = (1/r)(\partial P/\partial r)$  where  $P$  is the pressure, was solved as an eigenvalue of the problem. It should be noted that the magnitude of  $J$  is related to the stretch in the flame due to the imposed flow; as the magnitude of  $J$  increases, so does the strain rate. The strain rate SR was defined as  $SR = \sqrt{J/\rho_u}$ , where  $\rho_u$  is the density of the fresh gases.

The above system of coupled differential equations, described in greater detail in [13,14], must be closed with appropriate boundary conditions. Values for  $U$  and  $V$ ,  $Y_k$  and  $T$  were provided at the fresh reactant jet ( $x = 0$ ) and at the hot products jet ( $x = L = 1.486$  cm) as  $U(0) = U(L) = 0$ ;  $T(0) = T_u = 319$  K,  $T(L) = T_b$ . The equilibrium composition of the products of combustion at  $x = L$  was determined using the NASA Chemical Equilibrium Code CET93 [16] by calculating the chemical equilibrium of a  $\text{CH}_4/\text{air}$  mixture of equivalence ratio  $\varphi_b$  under conditions of constant temperature  $T = T_b$  and pressure of  $P = 1$  atm.

The differential equations were solved numerically using a phase-space, pseudo-arclength continuation method using as continuation variables the values of  $V$  at the two inlets. The set of equations given above was reparametrized using a new independent parameter  $s$  (pseudo-arclength), and the dependence of  $s$  on the remaining variables was specified by an extra scalar equation. The equations were discretized using finite differences, Newton-like iterations, and adaptive gridding. Within each Newton iteration, the linearized system has a block-tridiagonal sparsity structure and can be solved using an efficient direct solver. After each continuation step, the grid was refined by equidistributing a weight function that depends upon the gradient and curvature of all dependent variables [13,14].

In the present work, a methane mechanism [17] involving 46 species participating in 235 reversible reactions was employed. Comparison was made with the GRI 3.0 mechanism [18]. The GRI 3.0 mechanism tends to predict somewhat larger flame speeds and heat release. For example, in the case of a stoichiometric premixed flame opposed to stoichiometric products of combustion, the GRI 3.0 mechanism predicted an extinction strain rate 6% larger than that obtained with the reaction mechanism of UCSD [17]. However, results from the two mechanisms were not qualitatively different.

### 3. Results and discussion

The independent parameters of the counterflow problem (Fig. 1) are the equivalence ratios of the two opposed streams  $\varphi_u$  and  $\varphi_b$ , where the subscripts  $u$  and  $b$  refer to the unburnt reactant mixture and the burnt products, respectively, the temperature of the hot products stream  $T_b$  and the strain rate SR. To describe the composition of the two counterflowing streams, we used an abbreviated notation with two numbers: the first was the equivalence ratio of the fresh mixture and the second was the equivalence ratio  $\varphi_b$  of the premixed  $\text{CH}_4/\text{air}$  flame from which the equilibrium products of the counterflowing stream are generated. The latter is important since it indicates the presence of oxidizing species in the hot products or lack thereof. For example, 1.00/0.73 refers to a fresh reactant mixture of unity equivalence ratio counterflowing a hot product stream that is produced by a premixed flame of equivalence ratio 0.73. The temperature of the hot products was always 1800 K, unless otherwise specified. The notation 1.00/ $\text{N}_2$  refers to the presence of only  $\text{N}_2$  in the hot counterflowing stream. For all the flames, the temperature of the fresh reactant mixture  $T_u$  was fixed at 319 K and the pressure at one atmosphere.

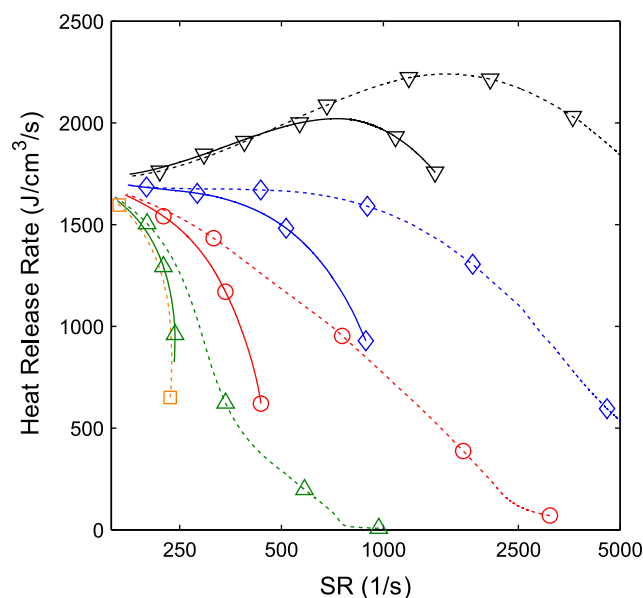
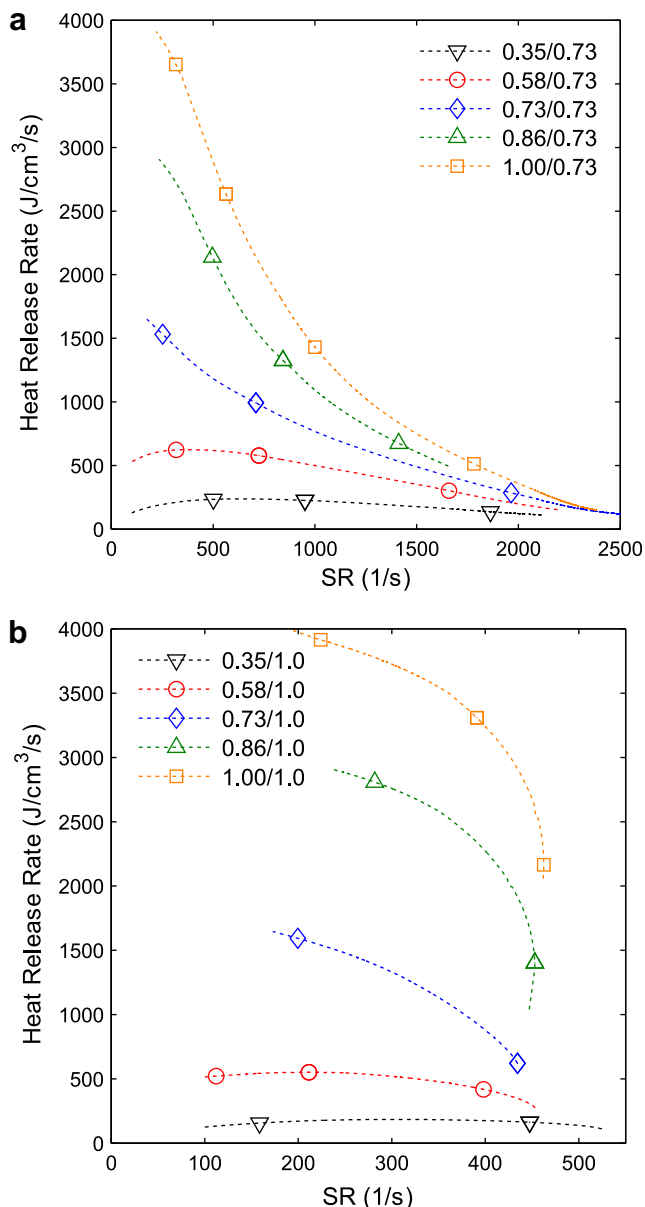


Fig. 2. Effect of strain rate on peak of heat release rate for different temperatures and compositions of the hot product stream and fixed composition of the reactant mixture at  $\varphi_u = 0.73$ . The composition effect is captured by the stoichiometry of the premixed flame generating the product stream, either  $\varphi_b = 0.73$  (dotted lines) or  $\varphi_b = 1.00$  (solid lines). Temperatures of the hot product stream are 1500 K ( $\square$ ), 1600 K ( $\triangle$ ), 1800 K ( $\circ$ ), 2000 K ( $\diamond$ ) and 2200 K ( $\nabla$ ). Curves are not interpolated but discrete symbols are used for clarity of presentation.

#### 3.1. Heat release and composition of counterflowing products of combustion

As illustrated in Fig. 2, the extinction behavior of a lean mixture of equivalence ratio 0.73 and adiabatic flame temperature 1900 K extinguishes abruptly if facing a stream of combustion products generated by a stoichiometric flame, in equilibrium at temperatures  $T_b$  of 1600 K, 1800 K, 2000 K or 2200 K. Whereas the same flame extinguishes smoothly in situations where the hot product stream originates from a lean flame of equivalence ratio  $\varphi_b = 0.73$  at those same temperatures. Furthermore, if the temperature  $T_b$  is further reduced to 1500 K, the dependence of the heat release rate on the strain rate takes a Z-shape. Similarly, Darabiha et al. [3] found that a propane/air premixed flame of equivalence ratio 0.75 facing the same fully-burnt reactant mixture extinguishes abruptly if the temperature  $T_b$  is set below 1530 K. Therefore, it can be qualitatively concluded that both conditions of elevated temperature and lean stoichiometry of the flame yielding these combustion products must be met for regimes of smooth extinction to take place. Consideration of the degree of non-adiabaticity alone is not sufficient to distinguish between smooth and abrupt extinction regimes. The effect of scalar stratification on the heat release rate of the fresh reactant mixture can be relatively severe. For instance, at  $T_b = 1800$  K, flame 0.73/1.00, close to extinction at  $SR = 440/\text{s}$ , generates nearly half as much heat as flame 0.73/0.73 at the same strain rate. We provisionally conclude that the so far neglected role of the hot product stream composition on the type of extinction experienced by the flame is just as critical as that of the temperature (and ensuing heat loss) associated with that stream.

With the previous observations in mind, the remainder of the article will explore further the effects of the equilibrium composition of the counterflowing combustion products at the temperature  $T_b$  maintained at a constant value of 1800 K. Fig. 3 considers the case in which the equivalence ratio of the fresh reactant mixture is now varied from 0.35 to 1.00 and the stoichiometry of the premixed flame feeding the hot product stream covers two cases:



**Fig. 3.** Effect of strain rate on peak of heat release rate for different stoichiometries of the fresh reactant mixture from  $\phi_u = 0.35$  to  $\phi_u = 1.00$  and fixed stoichiometry of the premixed flame generating the combustion products at a)  $\phi_b = 0.73$  and b)  $\phi_b = 1.00$ , respectively. Curves are not interpolated but discrete symbols are used for clarity of presentation.

a lean case at  $\phi_b = 0.73$  (Fig. 3a) and the stoichiometric case (Fig. 3b). Regardless of the stoichiometry of the fresh reactant mixture, the flame extinction is either smooth in the presence of lean counterflowing products of combustion or abrupt if the hot products are generated stoichiometrically. In the case of a smooth extinction, the peak of the heat release rate converges toward the same minimal value at large strain rates, which implies that the properties of the fresh mixture do not determine the burning rate under these highly strained conditions (Fig. 3a). In the case of abrupt flame extinction, the extinction strain rate would be expected to increase with the laminar flame speed or equivalently with the stoichiometry of the lean fresh mixture. Instead, the extinction strain rate was found to present a non-monotonic dependence on the equivalence ratio  $\phi_u$  (Fig. 3b): at first, as the equivalence ratio  $\phi_u$  is decreased from 1.00 to 0.73, the extinction strain rate decreases as anticipated. But the trend is reversed for

flames with  $\phi_u$  equal to 0.58 and 0.35. This behavior can be attributed to the super-adiabaticity that is experienced by the two leanest flames, whose adiabatic flame temperatures are lower than 1800 K. In agreement with [1], the value of the peak of heat release rate of the super-adiabatic flames at first was found to increase with strain rate, regardless of the stoichiometry of the counterflowing products, and ultimately smoothly decreases at the larger strain rates, or, for higher values of  $T_b$ , abrupt extinction occurs (Fig. 2).

Major species concentrations in the combustion products of premixed flames with equivalence ratios ranging from 0.73 to 1.00 are shown in Fig. 4. The concentrations of  $\text{CO}_2$  and  $\text{H}_2\text{O}$  in burnt products increase with the equivalence ratio in the examined lean branch, whereas that of  $\text{O}_2$  decreases to virtually zero at stoichiometric (Fig. 4a). Fig. 4b shows some minor species such as CO,

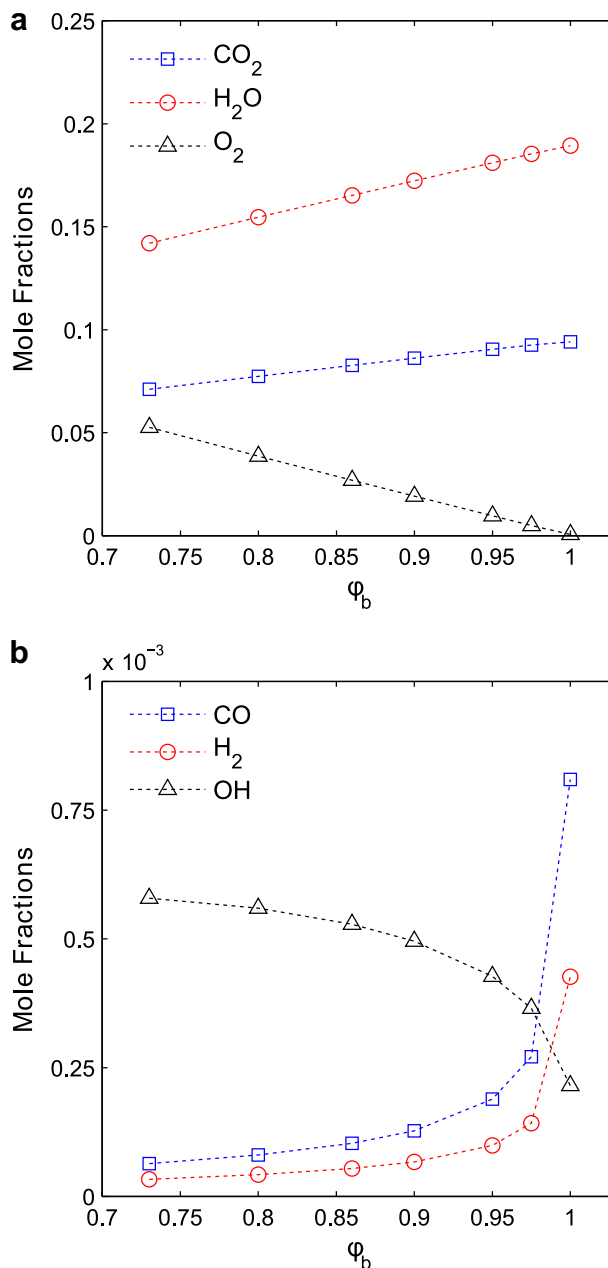


**Fig. 4.** Equilibrium concentrations of (a)  $\text{CO}_2$ ,  $\text{H}_2\text{O}$  and  $\text{O}_2$  and (b)  $\text{CO}$ ,  $\text{H}_2$  and  $\text{OH}$  in combustion products generated by premixed flames of equivalence ratios ranging from 0.73 to 1.00 at  $T_b = 1800$  K.

H<sub>2</sub> and OH, with the first two increasing with equivalence ratio and the last one showing an opposite trend. At the very large strain rates, when the flame is likely to be embedded in the stream of hot products, as will be seen in the next section, it is likely that minor species such as the OH radical in super-equilibrium in the burnt products of lean flames contributes to the smooth extinction behavior.

To assess in a conclusive fashion which species or group of species present in the counterflowing combustion products affect the type of extinction (smooth versus abrupt) most significantly and eliminate other chemical kinetic coupling effects, the simulation considered the “artificial” case of a stoichiometric mixture opposed to a hot nitrogen stream to which OH, O, H, H<sub>2</sub>, CO, CO<sub>2</sub>, H<sub>2</sub>O and O<sub>2</sub> were added one at a time in the same concentrations as in the  $\varphi_b = 0.73$  flame products, corresponding to the values under the leanest conditions in Fig. 3. Results are plotted in Fig. 5 showing that extinction is abrupt in all the cases at strain rates in the 400–600/s range, except for the case with the addition of O<sub>2</sub> for which extinction is reached at a significantly larger strain rate at nearly 1750/s. The flame 1.00/N<sub>2</sub> can be regarded as a reference case because of the chemical inertness of the counterflowing stream, as opposed to the others in which some degree of chemical reactions take place between fresh reactant and the hot gases. The Z-curves of the heat release rate of the flames with minor addition of OH, O, H, H<sub>2</sub> and CO to the N<sub>2</sub> stream are all overlapping with the 1.00/N<sub>2</sub> flame, which suggests that these species are at too small a concentration level to affect the rate of heat release of the strained premixed flame. With the addition of CO<sub>2</sub> or H<sub>2</sub>O to the N<sub>2</sub> stream, abrupt extinction happens at a lower strain rate than in the case of the counterflow flame 1.00/N<sub>2</sub>. CO<sub>2</sub> and H<sub>2</sub>O are gases with larger specific heats as compared to N<sub>2</sub> and therefore contribute more to lower the flame temperature. In addition, CO<sub>2</sub> and H<sub>2</sub>O in the otherwise inert stream tend to slow down the rate of product formation in the reaction zone. Consistent with Fig. 4a, we anticipated that this effect would become more pronounced with counterflowing products of stoichiometric flames since the concentrations of CO<sub>2</sub> and H<sub>2</sub>O in the burnt products increase with the equivalence

ratio. Clearly, the most dramatic effect is brought about by the addition of O<sub>2</sub> which is responsible for a dramatic increase of the extinction strain rate to a value nearly three times as large as in the 1.00/N<sub>2</sub> case and a smooth monotonic decrease of the heat release up to that point. In contrast, the addition of O<sub>2</sub> at the trace level corresponding to the products of a  $\varphi_b = 1.00$  flame at  $T_b = 1800$  K has virtually no effect on the extinction strain rate as compared to the reference case.

Conditions intermediate to those in Fig. 3 are presented in Fig. 6 showing the peak of heat release of a stoichiometric flame plotted against the strain rate for different compositions of the counterflowing products with  $\varphi_b$  ranging from 0.73 to 1.00. At low strain rate, the magnitude of the peak of heat release is the same for all cases, whereas distinct trends are observed above 395/s. A transition from abrupt extinction to a smooth one is observed when the flame yielding the equilibrium products of combustion is leaner than 0.9.

### 3.2. Burning regimes

The effect of the strain rate on the location of the peak of heat release is shown in Fig. 7, for the same combination of stoichiometries as in Fig. 6, namely stoichiometric fresh reactant stream and various lean stoichiometries of the flame yielding the combustion products. At low strain rate, the location of the peak of heat release and its magnitude (Fig. 6) are the same for all cases. The strained premixed flames propagate against the fresh reactant stream and stand away from the mixing layer at the stagnation plane. Increasing the strain rate tends to move the flame closer to the stagnation plane until the premixed flame front is forced to merge with the mixing layer at the stagnation plane. The effects of the equilibrium products of combustion become apparent when the peak of the heat release rate is located within 0.12 cm from the stagnation plane. In the case of abrupt extinction, as for flame 1.00/1.00, the location of the peak of the heat release rate remains on the fresh reactant side of the counterflow field up to extinction. A different scenario is experienced by the flames exhibiting a smooth extinction, as flame 1.00/0.73, for which the peak of the heat release crosses the stagnation plane and settles in the hot combustion

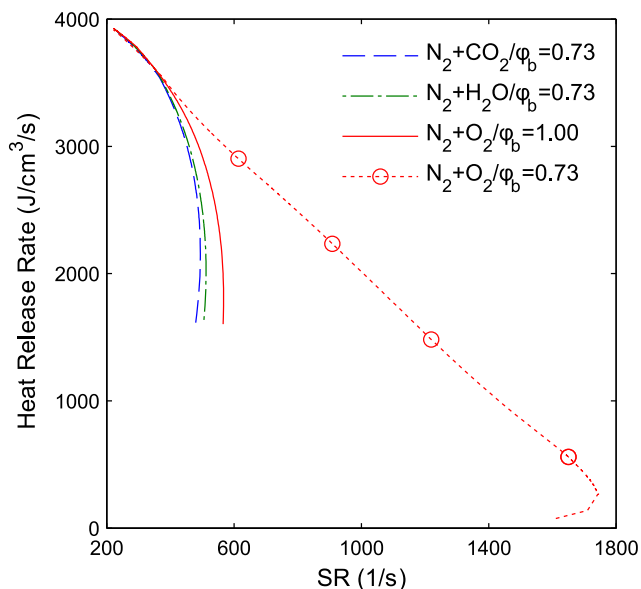


**Fig. 5.** Effect of strain rate on peak of heat release of a stoichiometric premixed flame opposed to a N<sub>2</sub> stream at 1800 K to which OH, O, H<sub>2</sub>, H, CO, CO<sub>2</sub>, H<sub>2</sub>O and O<sub>2</sub> are added one at a time at the same concentration as in the burnt products of a  $\varphi_b = 0.73$  flame. O<sub>2</sub> is also added at the same concentration as in the burnt products of a  $\varphi_b = 1.00$  flame. The solid line curve for N<sub>2</sub> + O<sub>2</sub>/ $\varphi_b = 1.00$  is indistinguishable from those pertaining to N<sub>2</sub> with the addition of OH, O, H<sub>2</sub>, H and CO. Curves are not interpolated but discrete symbols are used for clarity of presentation.

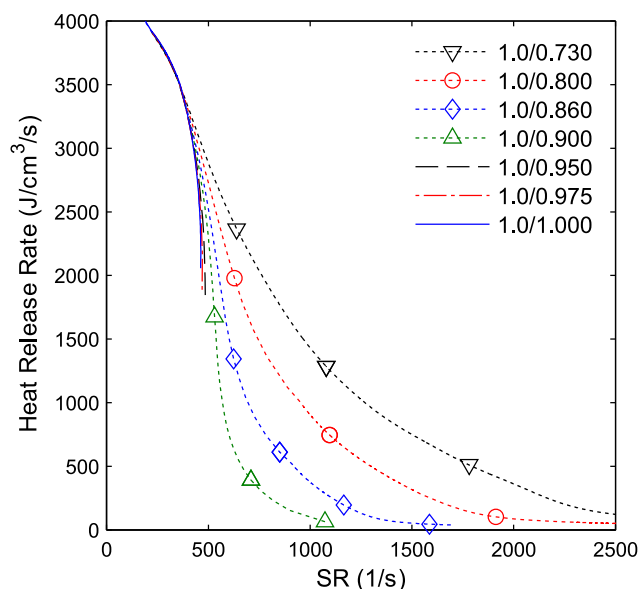


**Fig. 6.** Effect of strain rate on the heat release rate of stoichiometric mixture counterflow against products generated from lean-to-stoichiometric flames. Curves are not interpolated but discrete symbols are used for clarity of presentation.

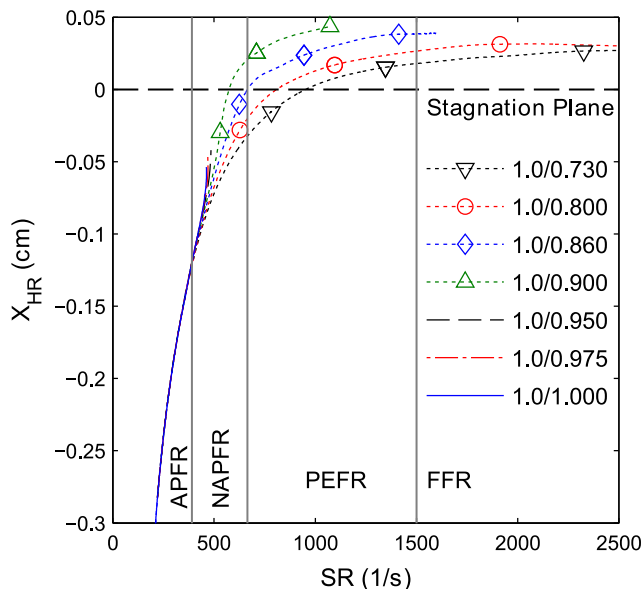


**Fig. 7.** Effect of strain rate on the location of the peak of heat release for the same composition combinations as in Fig. 6. Also labeled in the figure are various combustion regimes for flame 1.00/0.86: the adiabatic propagating flame regime (APFR), the non-adiabatic propagating flame regime (NAPFR), the so-called partially-extinguished flame regime (PEFR) and the frozen flow regime (FFR). Curves are not interpolated but discrete symbols are used for clarity of presentation.

product side at elevated strain rate. Under conditions of smooth extinction, four burning regimes can be distinguished as the strain rate is progressively increased: an adiabatic propagating flame regime (APFR), a non-adiabatic propagating flame regime (NAPFR), the so-called partially-extinguished flame regime (PEFR) and a frozen flow regime (FFR). The approximate ranges of strain rate pertaining to these regimes are also illustrated in Fig. 7 for flame 1.00/0.86.

Fig. 8 shows spatial temperature (solid line) and heat release (dashed line) profiles of flame 1.00/0.86 at  $T_b = 1800$  K and at four different strain rates corresponding to each of these burning regimes. The APFR regime corresponds to the low range of strain rate where the effects of the counterflowing products are not distinguishable, when the flame stands out of the mixing layer at the

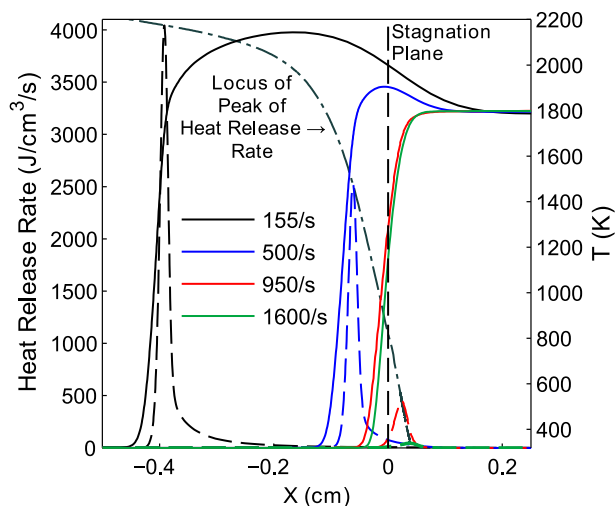


**Fig. 8.** Schematic of temperature profiles (solid lines) and heat release rate profiles (dotted lines) for flame 1.00/0.86 at  $T_b = 1800$  K, for the four different regimes in Fig. 7 that are established with increasing strain rates.

stagnation plane. In this regime, the magnitude of the peak of the heat release is virtually invariant with the strain rate. At intermediate strain rate, the NAPFR regime sets in, when the flame moves within the mixing layer straddling the stagnation plane, but still remains on the fresh reactant side of the stagnation plane. The effects of non-adiabaticity and of the composition of the hot products on the heat release become noticeable (Fig. 7). The flame still produces sufficient heat to sustain itself. If the system is sub-adiabatic, the temperature reaches a local maximum near the peak of heat release (Fig. 8). The peak temperature is reached nearer to the peak of the heat release and is lower than the adiabatic flame temperature of the fresh reactant mixture as a result of the volumetric heat loss on the burnt side. It decreases further as the strain rate is increased, until the temperature hump disappears and the temperature monotonically increases from the unburned side to the hot product side. In the super-adiabatic case, the temperature profile always remains monotonic, and the local temperature at the position of the peak of heat release increases with the strain rate until it reaches the temperature of the counterflowing gases. At an even larger strain rate, the PEFR regime appears when the peak of the heat release has crossed the stagnation plane. Once in the PEFR regime, the position of the flame, as indicated by the location of the peak of heat release, remains within the gas mixing layer and varies very gradually with the strain rate. In Fig. 8 ( $SR = 950/s$ ), the heat release, which has dropped by nearly one order of magnitude as opposed to what it was in the APFR regime, is too small for the flame temperature to exceed the one of the counterflowing gases. The flame cannot sustain itself and requires an external source of heat and oxidizer provided by the hot product stream. When the flame has moved to the hot side of the mixing layer, the concept of a negative displacement speed was put forth [1,19,20], but it may be somewhat misleading if one considers the intrinsically diffusive nature of the mixing between the fresh reactants and the hot products. At the highest strain rates, when the heat release rate approaches zero, the flame temperature profile is practically identical to that ensuing from the non-reacting mixing of two streams at different temperatures. We refer to this situation as the FFR regime, since chemistry is essentially inactive. In ultra-lean mixtures as with flame 0.35/0.73 in Fig. 3a, the APFR and NAPFR regimes are not present, since these flames do not propagate and for all intents and purposes they are like partially premixed diffusion flames.

### 3.3. Structure of the flame with strain rate

The multilayer structure of a freely propagating methane premixed flame is well established in the context of a reaction rate asymptotic analysis (e.g., [5]) and can provide some guidance in understanding the effect of strain and composition of the hot product stream. The premixed flame is composed of a preheat zone, a fuel consumption layer and an oxidation layer. In the preheat zone, the gas temperature is below the threshold for chemical reactions to take place. The fuel is attacked in the fuel consumption layer by the H, OH and O radicals to yield CO, with the main reaction pathway serially including the intermediate species  $CH_3$ ,  $CH_2O$ , and HCO. In the oxidation layer, CO is further oxidized by the OH radical to form  $CO_2$  via reaction  $CO + OH = CO_2 + H$  and, to a lesser extent, the oxidation of  $H_2$  to  $H_2O$  is completed.

Fig. 9a and c shows the concentrations and chemical production rates of some critical species for Flame 1.00/0.86 in the APFR regime at  $SR = 175/s$ . The abscissa origin is the location of the peak of the heat release rate that coincides with that of HCO [21]. The relatively narrow fuel consumption layer, arbitrarily defined in Fig. 9c as the full width at 10% of maximum of the  $CH_4$  consumption rate, straddles the location of the peaks of  $H_2$ , HCO and CO concentrations. To the right of the origin is the relatively thick oxi-

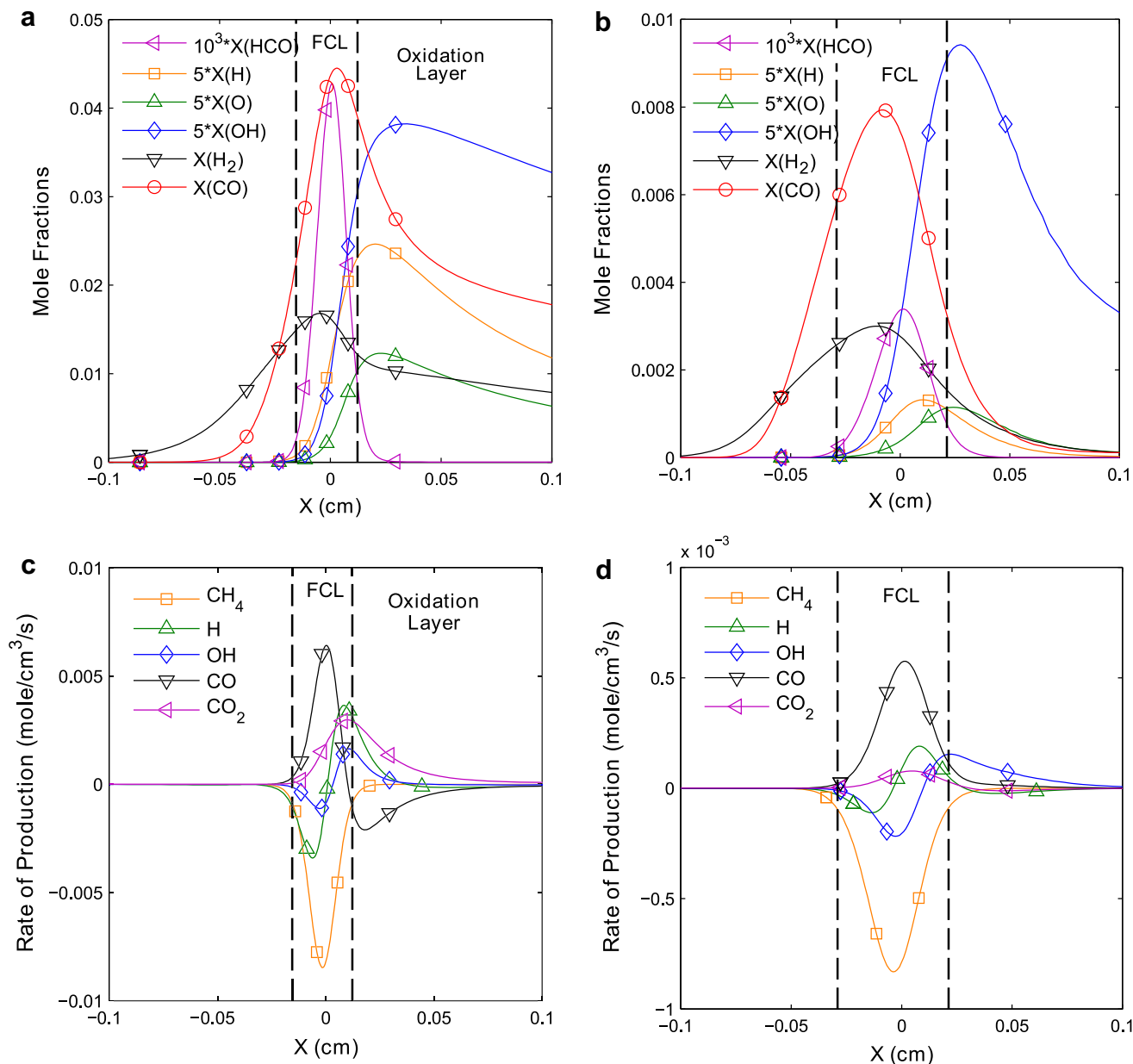


**Fig. 9.** Structure of the fuel consumption layer and oxidation layer in Flame 1.00/0.86 at SR = 175/s (a and c) and SR = 1100/s (b and d): mole fractions of H, O, OH, H<sub>2</sub>, HCO and CO (a and b); production rates of CH<sub>4</sub>, CO<sub>2</sub> and some critical intermediates (H, OH, CO) (c and d). In each plot, the vertical dashed lines mark the boundary of the fuel consumption layer (FCL), as determined by the full width at 10% of maximum of CH<sub>4</sub> consumption rate. Notice scale factors in the legends of H, O, OH and HCO mole fractions in (a and b) and the change in y-axis scale between plots at SR = 175/s and SR = 1100/s. Curves are not interpolated but discrete symbols are used for clarity of presentation.

oxidation layer within which the oxidation of CO and H<sub>2</sub> are completed. Fig. 9b and d shows how the structure of the flame is changed in the PEFR regime at SR = 1100/s. Compared to the flame at SR = 175/s, the mole fractions of the species plotted in Fig. 9b are all significantly decreased, although comparatively CO, H<sub>2</sub> and OH are less depleted. The fuel consumption layer also became broader at SR = 1100/s. In Fig. 9c, CO is being produced within the fuel consumption layer and being consumed in the oxidation layer. However, in the PEFR regime (Fig. 9d), CO, though still produced in the fuel consumption layer, is no longer consumed in the oxidation layer. As a result, the production rate of CO<sub>2</sub>, which straddles the fuel consumption layer and the oxidation layer at low strain rate, practically vanishes in the PEFR regime, as shown by the production rates plotted in Fig. 9d.

Fig. 10 shows how the concentrations of the H, OH and O radicals as well as of the CO and H<sub>2</sub> intermediate species are depleted

as the strain rate increases. All values are normalized with those at SR = 220/s. Two flames are compared: 1.00/1.00 and 1.00/0.73, with abrupt extinction in the first case and smooth extinction in the second case. With increasing strain rate, the concentrations of all the species and radicals decrease. Yet, depending on the composition of the counterflowing gases, some species and radicals in the flame tend to be depleted faster than others. In the case of flame 1.00/1.00 (Fig. 10a), the three radicals H, O and OH are all equivalently depleted by the strain rate, up to the onset of abrupt extinction. CO and H<sub>2</sub> comparatively resist better to the increase in strain rate because these species are produced in the fuel consumption layer and consumed in the oxidation layer (Fig. 9a and c). The abrupt extinction can therefore be attributed to the partial quenching of the oxidation layer, as was pointed out in the discussion in Fig. 9. The present evidence suggests that the entire H–OH–O radical pool is comparably affected. However, in the case of flame

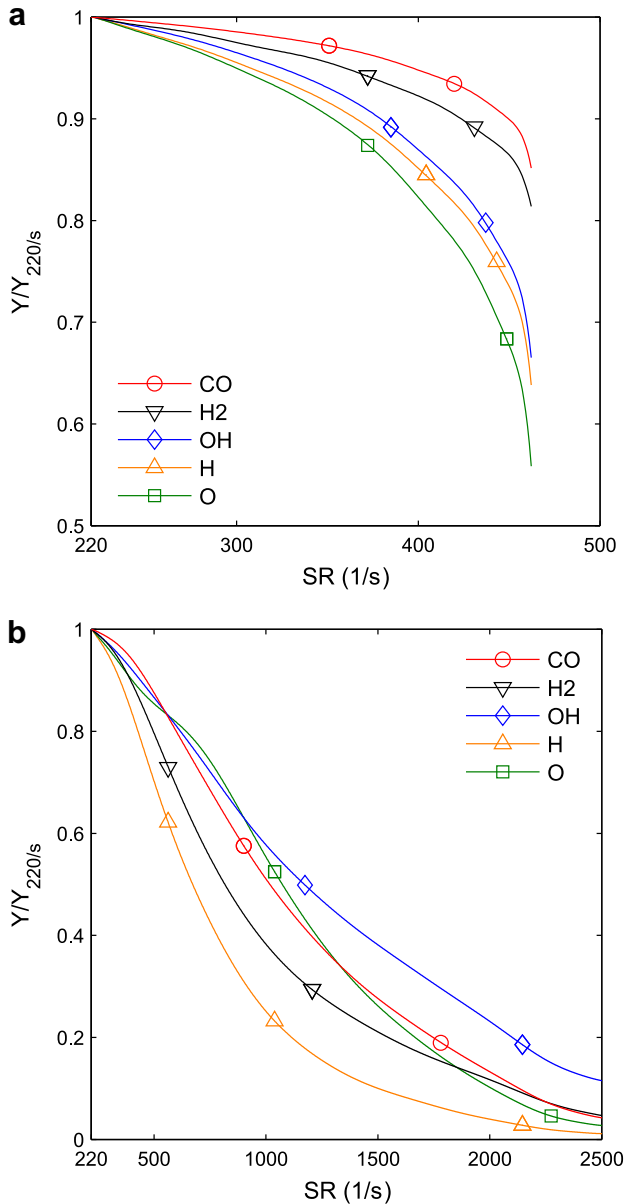


**Fig. 10.** Effect of strain rate on the peak concentration of key radicals H, O, OH, H<sub>2</sub> and CO normalized by the corresponding values at SR = 220/s for flames (a) 1.00/1.00 and (b) 1.00/0.73. Curves are not interpolated but discrete symbols are used for clarity of presentation.

1.00/0.73 (Fig. 10b) which exhibits a smooth extinction, the H radical is the most depleted of all the radicals with increasing strain rate. OH remains abundant by comparison.

To provide the necessary context, it is worthwhile to recall that some important reaction steps of methane oxidation:



are critical chain-branching steps contributing to the formation of the H, O and OH radicals. The dominant attack on the fuel is by the H and OH radicals according to



and



CO is essentially produced by reaction:



where M refers to a third body, and then CO is finally converted to CO<sub>2</sub> by the OH radical according to the reaction



extending in the oxidation layer. These last two reactions also contribute to the formation of H. Fig. 11 shows the net reaction rates for flame 1.00/0.86 at strain rates 175/s (Fig. 11a) and 1100/s (Fig. 11b), corresponding to the APFR regime and EPFR regime, respectively. At low strain rate (Fig. 11a), all these reactions are active with their peaks in the fuel consumption layer. When the flame has moved to the other side of the stagnation plane (Fig. 11b), reactions (2), (3), and (7), which contribute to produce the H radical, are particularly affected by comparison with the other reactions listed above.

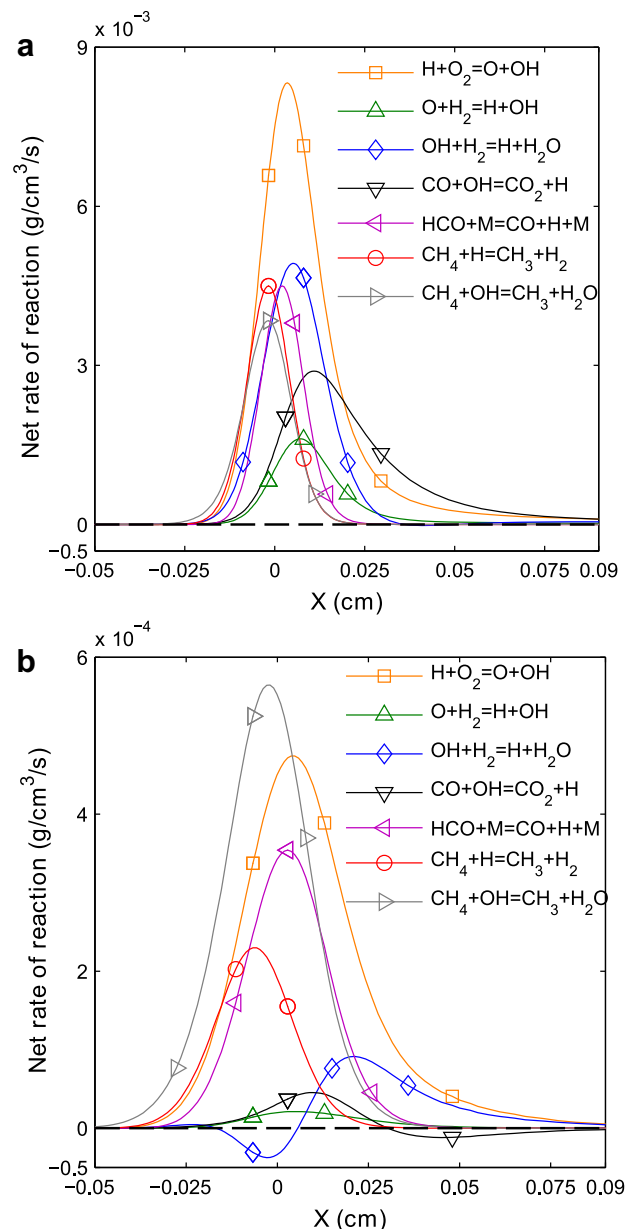


**Fig. 11.** Dominant reactions in flame 1.00/0.86 at  $T_b = 1800$  K. The net reaction rates are plotted in the flame reference frame: (a) APFR regime at SR = 175/s and (b) PEFR regime at SR = 1100/s. Curves are not interpolated but discrete symbols are used for clarity of presentation.

Reactions (2) and (7) are quenched and (3) tends to be driven backward consuming the H radical. Furthermore, the presence of H<sub>2</sub>O and CO<sub>2</sub> in the counterflowing gases tends to favor the backward reactions in (3) and (7). At the same time, reaction (6) that dominates the production of the H radical in the fuel consumption layer at low strain rate remains active relative to the other reactions as the strain rate increases. Consequently, after the quenching of the oxidation layer at large strain rate, the production of H radical shifts upstream, as is also noticeable in Fig. 9d. In Fig. 11b, it appears that OH dominates the attack of the fuel via reaction (5). At high strain rate, the OH radical is directly fed into the reaction zone by the lean counterflowing products of combustion (Fig. 4b). The OH radical also benefits from the increase in the backward rate of (3) and the quenching of (7), consuming the OH radical. In addition, reaction (1), which is still active at high strain rates thanks to the presence of O<sub>2</sub> in the counterflowing hot products, continues to contribute to the production of OH.

At the highest strain rates, at the onset of the frozen flow regime, the pool of H and O radicals has vanished (Fig. 9b), and the production rate of the OH radical has also significantly decreased. The flame finds a source of radicals via diffusion from the hot products, where particularly the OH radical is stable at high temperature. Consequently, the fuel consumption is still carried out dominantly by reaction (5), which becomes the principal source of H<sub>2</sub>O and of the weak heat release rate at those high strain rates. Since the radical pool is drastically reduced, CH<sub>3</sub> is produced at a larger rate than it is consumed, and its concentration in the reaction zone reaches a plateau.

#### 4. Implications for premixed turbulent combustion

Within a flamelet approach to turbulent combustion, there is an obvious link between the present study on the burning rate of laminar flames and turbulent combustion, since the structure of a turbulent flame is not fundamentally different from that of a laminar one, up to the onset of extinction [5]. Within the flamelet regime, the flame front remains singly connected and it acts as a thin interface between reactants and products. In the non-flamelet regime, also referred to as broken reaction zones regime or distributed flame fronts regime, the turbulent flame front is locally extinguished by the turbulent eddies. This regime is anticipated under very intense turbulence in some practical applications, such as homogeneous charge compression ignition engines, industrial furnaces, supersonic combustors and, possibly, stationary gas turbines for power generation. The boundary between the flamelet regime and the non-flamelet one is traditionally defined in terms of a turbulent Karlovitz number  $Ka_\eta$ , that is the ratio of a relevant chemical timescale to the turn-over time of the Kolmogorov microscale.  $Ka_\eta$  quantifies the degree of turbulence/chemistry interaction [22]. When it attains sufficiently large values, turbulent premixed combustion transitions from one regime to the other. It is important to realize that this classification and the accompanying diagram of turbulent combustion, the so-called Borghi diagram, was conceived for homogeneous reactant mixtures and self-sustained freely propagating turbulent flames.

There are two additional ingredients in common between turbulent combustion and the present problem. First, the presence of heat loss/gain, which was simulated with an independent control of the temperature of the hot product stream, mimics the volumetric heat loss in the vicinity of surfaces in practical systems. The effect of heat loss (gain) is known to displace the limit of the flamelet regime to lower (higher) values of the turbulent Karlovitz number [23]. For example, consistent with the results of Section 3, we anticipated that at the onset of the non-flamelet regime, a near-stoichiometric flame would undergo abrupt local extinctions,

whereas a lean flame is more likely to exhibit partially extinguished conditions and a wider range of burning rates. Second, the unburnt mixture may interact in the same combustor with hot products generated from a flame with a locally different stoichiometry. The burning of a turbulent stratified flame in which there is a gradient of equivalence ratio along the flame is typical of situations requiring near-stoichiometric burning in the vicinity of the fuel injector for robust flame stabilization and an overall lean, or even ultra-lean, stoichiometry in the combustion chamber to minimize pollutant emission. Pilot flames, swirl or bluff-bodies are routinely used in practical combustors and laboratory flames to promote mixing of the reactants with hot combustion products and stabilize premixed turbulent flames [24–32]. Because of the effects of the high temperature and the composition of the stabilizing combustion products, the so called Borghi diagram [22], that provides a framework for the understanding of various turbulent combustion regimes, does not permit to predict even qualitatively the burning regime of these flames. Under these conditions, as illustrated in the present article, the extinction behavior and the definition of the boundary of the flamelet regime are affected not only by heat loss/gain, but also by the local composition of the hot products, especially with respect to the presence of oxidizing species.

As it was mentioned in the introduction, the reactant-to-product flamelet model was found to perform well in predicting the burning rate statistics of adiabatic turbulent premixed flames [7]. The present study suggests that this configuration could also be used as a relevant flamelet model for the prediction of burning rates in stratified turbulent combustion.

Even within a one-step chemical kinetic theory of premixed flame that neglects any complications stemming from chemical kinetics, if conditions are such that pockets of fluids originating from mixtures at various equivalence ratios interact, there are, in principle, at least as many chemical timescales in the problem, which, in turn, results in the determination of multiple Karlovitz numbers. It is clear, then, that the Borghi diagram, while useful in framing a first order description of the rich field of turbulent premixed combustion, is inadequate to capture these subtle, yet practically relevant, distinctions.

To shed light on these issues, experimental studies are under way in a highly turbulent counterflow burner in which one jet of fresh reactants is opposed to a second jet of hot combustion products whose temperature and composition can be independently controlled [12]. A systematic study of the local flame structure in these premixed turbulent environments at elevated turbulent Reynolds numbers and over a wide range of Karlovitz numbers is under way.

#### 5. Conclusions

The extinction of premixed CH<sub>4</sub>/air flames counterflowing against a jet of combustion products in chemical equilibrium at high temperatures was investigated numerically using detailed chemistry and transport mechanisms. Controlled independent variables included the fresh reactant composition and the composition of the hot product stream. Contrary to similar studies of this type that were focused on heat loss/gain from the hot product stream, the emphasis was on the yet unexplored role of the composition of the counterflowing combustion products on the extinction of lean-to-stoichiometric premixed flames. The topic is relevant to practical combustion applications in which near-stoichiometric conditions are established near the fuel injector for flame stabilization purposes, whereas the flame is progressively leaned out further downstream to meet pollution restrictions.

Two distinct extinction modes were observed: an abrupt one, when the hot counterflowing stream consists of either inert gas

or equilibrium products of a stoichiometric premixed flame, and a smooth extinction, when there is an excess of oxidizing species in the combustion product stream.

Under conditions of smooth extinction, four burning regimes can be distinguished as the strain rate is progressively increased: an adiabatic propagating flame regime, a non-adiabatic propagating flame regime, the so-called partially-extinguished flame regime, and a frozen flow regime.

Abrupt extinction was attributed to the quenching of the oxidation layer with the entire H–OH–O radical pool being comparably reduced. Under conditions of smooth extinction, the behavior is different and the concentration of the H radical decreases the most with increasing strain rate, whereas OH and O remain comparatively abundant in the oxidation layer. The production of H radical is shifted towards the reactants in the partially-extinguished regime, whereas the production rates of OH and O are slightly shifted in the opposite direction, yielding a thickening of the profile of heat release rate. Under these conditions, the oxidation layer is quenched, but the structure of the flame relies more heavily on the preferential use of the OH radical.

### Acknowledgments

The authors gratefully acknowledge the financial support of ACS/PRF (Grant #FA9550-06-1-0018). We are thankful to Drs. Beth A.V. Bennett and Seth Dworkin for their help with the use of the arc length continuation code and to Mr. Brian Dobbins for his support with the computational facilities.

### References

- [1] P.A. Libby, F.A. Williams, *Combust. Sci. Technol.* 31 (1983) 1–42.
- [2] N. Darabiha, S.M. Candel, F.E. Marble, *Combust. Flame* 64 (1986) 203–217.
- [3] N. Darabiha, S.M. Candel, V. Giovangigli, M.D. Smooke, *Combust. Sci. Technol.* 60 (1988) 267–285.
- [4] B. Rogg, *Combust. Flame* 73 (1988) 45–65.
- [5] F.A. Williams, *Prog. Energy Combust. Sci.* 26 (2000) 657–682.
- [6] P.A. Libby, F.A. Williams, *Combust. Flame* 44 (1982) 287–303.
- [7] E.R. Hawkes, J.H. Chen, *Combust. Flame* 144 (2006) 112–125.
- [8] H.N. Najm, P.S. Wyckoff, *Combust. Flame* 110 (1997) 92–112.
- [9] E. Mastorakos, A.M.K. Taylor, J.H. Whitelaw, *Combust. Flame* 102 (1995) 101–114.
- [10] Y.M. Marzouk, A.F. Ghoniem, H.N. Najm, *Proc. Combust. Inst.* 28 (2000) 1859–1866.
- [11] T. Kang, D.C. Kyritsis, *Proc. Combust. Inst.* 31 (2007) 1075–1083.
- [12] B. Coriton, J.H. Frank, A.G. Hsu, M.D. Smooke, A. Gomez, *Proc. Combust. Inst.*, vol. 33, 2010, in press.
- [13] M.D. Smooke, J. Crump, K. Seshadri, V. Giovangigli, *Proc. Combust. Inst.* 23 (1990) 463–470.
- [14] V. Giovangigli, M.D. Smooke, *J. Comp. Physiol.* 68 (1987) 327–345.
- [15] V. Giovangigli, N. Darabiha, in: *Proceedings of the Conference on Mathematical Modeling in Combustion*, April 1987, Lyon, France, NATO ASI Series.
- [16] S. Gordon, B.J. McBride, NASA TM-4557, 1994.
- [17] “Chemical-Kinetic Mechanisms for Combustion Applications”, San Diego Mechanism web page, Mechanical and Aerospace Engineering (Combustion Research), University of California at San Diego <<http://maeweb.ucsd.edu/combustion/cermec/>> (accessed 07/2009).
- [18] G.P. Smith, D.M. Golden, M. Frenklach, N.W. Moriarty, B. Eiteneer, M. Goldenberg, C.T. Bowman, R.K. Hanson, S. Song, W.C. Gardiner, Jr., V.V. Lissianski, Z. Qin, <[http://www.me.berkeley.edu/gri\\_mech/](http://www.me.berkeley.edu/gri_mech/)> (accessed 07/2009).
- [19] Z. Cheng, J.A. Wehrmeyer, R.W. Pitz, *Proc. Combust. Inst.* 30 (2005) 285–293.
- [20] I.R. Gran, T. Echehki, J.H. Chen, *Proc. Combust. Inst.* 26 (1996) 323–329.
- [21] H.N. Najm, P.H. Paul, C.J. Mueller, P.S. Wyckoff, *Combust. Flame* 113 (1998) 312–332.
- [22] N. Peters, *Turbulent Combustion*, Cambridge Monographs on Mechanics, Cambridge University Press, Cambridge, United Kingdom, 2000.
- [23] T. Poinsot, D. Veynante, S. Candel, *J. Fluid Mech.* 228 (1991) 561–606.
- [24] M.S. Mansour, N. Peters, Y.C. Chen, *Proc. Combust. Inst.* 27 (1998) 767–773.
- [25] V. Robin, A. Mura, M. Champion, O. Degardin, B. Renou, M. Boukhalfa, *Combust. Flame* 153 (2008) 288–315.
- [26] A.X. Sengissen, A.V. Giauque, G.S. Staffelbach, M. Porta, W. Krebs, P. Kaufmann, T.J. Poinsot, *Proc. Combust. Inst.* 31 (2007) 1729–1736.
- [27] R.S. Barlow, G.-H. Wang, P. Anselmo-Filho, M.S. Sweeney, S. Hochgreb, *Proc. Combust. Inst.* 32 (2009) 945–953.
- [28] M.J. Dunn, A.R. Masri, R.W. Bilger, R.S. Barlow, G.-H. Wang, *Proc. Combust. Inst.* 32 (2009) 1779–1786.
- [29] K.-J. Nogenmyr, C. Fureby, X.S. Bai, P. Peterson, M. Linne, *Combust. Flame* 156 (2009) 25–36.
- [30] I. Boxx, M. Stöhr, C. Carter, W. Meier, *Combust. Flame* (2010). [10.1016/j.combustflame.2009.12.015](https://doi.org/10.1016/j.combustflame.2009.12.015).
- [31] S. Chaudhuri, S. Kostka, M.W. Renfro, B.M. Cetegen, *Combust. Flame* (2010). doi:10.1016/j.combustflame.2009.10.020.
- [32] F. Seffrin, F. Fuest, D. Geyer, A. Dreizler, *Combust. Flame* 157 (2010) 384–396.